Near-infrared light scattering by particles in coastal waters

David Doxaran, Marcel Babin, Edouard Leymarie

▶ To cite this version:

HAL Id: hal-02539765
https://hal.sorbonne-universite.fr/hal-02539765

Submitted on 30 Dec 2023

Near-infrared light scattering by particles in coastal waters

David Doxaran[*], Marcel Babin and Edouard Leymarie

Université Pierre et Marie Curie - Paris 6, Laboratoire d'Océanographie de Villefranche, Villefranche-sur-Mer,
France – Centre National de la Recherche Scientifique (CNRS)
doxaran@obs-vlfr.fr

Abstract: We report the first measurements of the scattering coefficient of natural marine particles, which extend over the near-infrared spectral region to up to 870 nm. The measurements were conducted in three different European estuaries (Gironde, Tamar and Elbe) using an in situ absorption and attenuation-meter. The observed particulate scattering coefficients varied from 1 to nearly 100 m^{-1}. The spectral shape in the near-infrared very closely matched a $\lambda^{-\gamma}$ spectral dependence, which is expected when the particle size followed a power-law distribution. The spectral slope of the scattering spectrum, γ, spanned from 0.1 to 1.2 and showed significant regional and temporal variations. These variations were certainly related to the particle size distribution, which will have to be studied in future works. Using our near-infrared data as a reference, we assessed the use of the attenuation coefficient spectrum in the visible range to estimate the near-infrared particulate scattering slope and found values different by 10% on average.

References and links

1. A. Bricaud, C. Roesler, and J.R.V. Zaneveld, "In situ methods for measuring the inherent optical properties of ocean waters," Limnol.Oceanogr. **40**, 393-410 (1995).
2. M. Babin, A. Morel, V. Fournier-Sicre, F. Fell, and D. Stramski, "Light scattering properties of marine particles in coastal and oceanic waters as related to the particle mass concentration," Limnol. Oceanogr. **48**, 843-859 (2003).
3. M. Defoin Platel, and M. Chami, "How ambiguous is the inverse problem of ocean color in coastal waters," J.Geophys. Res. **112**, doi10.1029/2006JC003847 (2007).
4. B. G. Mitchell, and M. Kahru, "Algorithms for SeaWiFS standard products developed with the CalCOFI bio-optical data set," Calif. Coop. Oceanic Fish. Invest. Rep. **39**, 133-147 (1998).
5. D. Doxaran, J. M. Froidefond, and P. Castaing, "Remote sensing reflectance of turbid sediment- dominated waters. Reduction of sediment type variations and changing illumination conditions effects using reflectance ratios," Appl. Opt. **42**, 2623-2634 (2003).
6. N. V. Blough, and R. Del Vecchio, "Chromophoric dissolved organic matter (CDOM) in the coastal environment," in *Biogeochemistry of Marine Dissolved Organic Matter*, D. Hansell and C. Carlson, eds., (Academic Press, San Diego, 2002) pp. 509–546.
7. A. Morel, B. Gentili, H. Claustre, M. Babin, A. Bricaud, J. Ras, and F. Tieche, "Optical properties of the "clearest" natural waters," Limnol. Oceanogr. **52**, 217-229 (2007).
8. I. Laurion, F. Blouin, and S. Roy, "The quantitative filter technique for measuring phytoplankton absorption: interference by MAAS in the UV waveband," Limnol. Oceanogr. **1**, 1-9 (2003).
9. R. M. Pope, and E. S. Fry, "Absorption spectrum (380–700 nm) of pure water," Appl. Opt. **36**, 8710–8723 (1997).
10. V. S. Langford, A. J. McKinley, and T. I. Quickenden, "Temperature dependence of the visible-near-infrared absorption spectrum of liquid water," J. Phys. Chem. A **105**, 8916-8921 (2001).
11. M. Babin, and D. Stramski, "Light absorption by aquatic particles in the near-infrared spectral region," Limnol. Oceanogr. **47**, 911-915 (2002).
12. M. Babin and D. Stramski, "Variations in the mass-specific absorption coefficient of mineral particles suspended in waters," Limnol. Oceanogr. **49**, 756-767 (2004).

13. S. Tassan and G. M. Ferrari, "Variability of light absorption by aquatic particles in the near-infrared spectral region," Appl. Opt. **42**, 4802-4810 (2003).
14. A. Morel, "Diffusion de la lumière par les eaux de mer. Résultats expérimentaux et approche théorique. Optics of the sea," AGARD Lectures Series (1973).
15. A. Morel, "Optical modeling of the upper Ocean in relation to its biogenous matter content (case I waters)," J. Geophys. Res. **93**, 10749-10768 (1988).
16. S. Maritorena, D. A. Siegel, and A. R. Peterson, "Optimization of a semianalytical ocean color model for global-scale applications," Appl. Opt. **41**, 2705-2714 (2002).
17. G. F. Moore, J. Aiken, and S. J. Lavender, "The Atmospheric correction of water colour and the quantitative retrieval of suspended particulate matter in Case II Waters: application to MERIS," Int. J. Remote Sens. **20**, 1713-1733 (1999).
18. M. Jonasz and G. R. Fournier, "Approximation of the size distribution of marine particles by a sum of log-normal functions," Limnol. Oceanogr. **41**, 744-754 (1996).
19. W. S. Pegau, D. Gray, and J. R. V. Zaneveld, "Absorption and attenuation of visible and near-infrared light in water: dependence on temperature and salinity," Appl. Opt. **36**, 6035-6046 (1997).
20. J. M. Sullivan, M. S. Twardowski, J. R. V. Zaneveld, C. M. Moore, A. H. Barnard, P. L. Donaghay, and B. Rhoades, "Hyperspectral temperature and salt dependence of absorption by water and heavy water in the 450-750 nm spectral range," Appl. Opt. **45**, 5294-5309 (2006).
21. J. R. V. Zaneveld, J. C. Kitchen, and C. C. Moore, "Scattering error correction of reflecting tube absorption meters," Proc. SPIE **2258**, 44-55 (1994).
22. C. S. Roesler and E. Boss, "A novel ocean color inversion model: retrieval of beam attenuation and particle size distribution,"Geophys. Res. Let. **30**, 10.1029/2002GL016366 (2003).
23. J.-F. Berthon, Joint Research Centre, European Commission, Ispra, Italy, (personal communication, 2006).
24. A. L. Whitmire, E. Boss, T. J. Cowles, and W. S. Pegau, "Spectral variability of the particulate backscattering ratio," Opt. Express **15**, 7019-7031 (2007).
25. R. C. Smith and K. S. Baker, "Optical properties of the clearest natural waters (200-800nm). Appl. Opt. **20**, 177-184 (1981).
26. D. McKee, A. Cunningham, and S. Craig, "Semi-empirical correction algorithm for ac-9 measurements in a coccolithophore bloom," Appl. Opt. **42**, 4369-4374 (2003).
27. M. Chami, E. B. Shybanov, G. A. Khomenko, M. E. G. Lee, O. V. Martynov, and G. K. Korotaev, "Spectral variation of the volume scattering function measured over the full range of scattering angles in a coastal environment," Appl. Opt. **45**, 3605-3619 (2006).
28. J. Piskozub, D. Stramski, E. Terril, and W. K. Melville, "Influence of forward and multiple light scatter on the measurements of beam attenuation in highly scattering marine environments," Appl. Opt. **43**, 4723-4731 (2004).
29. E. Leymarie, Université Pierre et Marie Curie Paris 6 - CNRS, Laboratoire d'Océanographie de Villefranche, Villefranche-sur-Mer, France (personal communication, 2006).
30. T. J. Petzold, "Volume scattering functions for selected ocean waters," Scripps Institution of Oceanography. Ref. 72-78, 79 pp (1972).
31. A. H. Barnard, W. S. Pegau, and J. R. V. Zaneveld, "Global relationships of the inherent optical properties of the oceans," J. Geophys. Res. **75**, 2837-2845 (1998).
32. R. W. Gould, R. Arnone, and P. M. Martinolich, "Spectral dependence of the scattering coefficient in case 1 and case 2 waters," Appl. Opt. **38**, 2377-2383 (1999).
33. C. D. Mobley, *Light and Water, Radiative Transfer in Natural Waters* (Academic, 1994).
34. H. Bader, "The hyperbolic distribution of particle sizes," J. Geophys. Res. **75**, 2822-2830 (1970).
35. R. W. Sheldon, "Size separation of marine seston by membrane and glass-fiber filters," Limnol. Oceanogr. **17**, 494-498 (1972).
36. M. Jonasz, "Particle size distributions in the Baltic," Tellus B **35**, 346-358 (1983).
37. G. A. Jackson, R. E. Maffione, D. K. Costello, A. L. Alldredge, B. E. Logan, and H. G. Dam, "Particle size spectra between 1μm and 1cm at Monterey Bay determined using multiple instruments," Deep-Sea Res. **44**, 1739-1768 (1997).
38. E. Boss, W. S. Pegau, W. D. Gardner, J. R. V. Zaneveld, A. H. Barnard, M. S. Twardowski, G. C. Chang, and T. D. Dickey, "Spectral particulate attenuation and particulate size distribution in the boundary layer of a continental shelf," J. Geophys. Res. **106**, 9509-9516 (2001).
39. E. Boss, M. S. Twardowski, and S. Herring, "Shape of the particulate beam attenuation spectrum and its inversion to obtain the shape of the particulate size distribution," Appl. Opt. **40**, 4885-4893 (2001).
40. S. J. Lavender, M. H. Pinkerton, G. F. Moore, J. Aiken, and D. Blondeau-Patissier, "Modification to the Atmospheric Correction of SeaWiFS Ocean Colour Images over Turbid Waters," Cont. Shelf Res. **25**, 539-555 (2005).
41. K. G. Ruddick, V. De Cauwer, Y. J. Park, and G. F. Moore, "Seaborne measurements of near infrared water-leaving reflectance: The similarity spectrum for turbid waters," Limnol. Oceanogr. **51**, 1167-1179 (2006).

1. Introduction

The modeling of light propagation in the ocean requires knowledge about trends in the variability of inherent optical properties (IOPs) of seawater, and dissolved and particulate substances it contains. Measurements made in the laboratory have contributed to document IOPs of the major seawater optically significant constituents, especially phytoplankton, but the major steps forward were accomplished thanks to large data sets of IOPs measured on natural samples. Recent studies on the absorption coefficient of phytoplankton and the scattering coefficient of suspended particles are examples of such steps forward [1-2].

Most of what we know today on seawater IOPs concerns the visible part of the spectrum. As we approach the limit in the amount of information that can be extracted from that spectral range on seawater composition and processes [3], the ultraviolet (UV) and near-infrared (near-IR) domains are now explored (e.g. [4-5]). In the UV range, while the absorption spectrum of colored dissolved organic matter has been relatively well documented [6], uncertainties about pure seawater absorption remain [7] and the absorption coefficient of particles is poorly documented [8]. In the near-IR spectral region, while the absorption coefficient of pure seawater is relatively well documented [9-10], and uncertainties remain about absorption by particles because of experimental difficulties [11-13], no measurement of the scattering coefficient of natural marine particles has yet been reported in the literature.

The near-IR region is of significant interest because the interpretation of IOPs in that spectral region may prove to be relatively simple, and informative with regards to suspended particles [5]. Indeed, in that spectral region, IOPs as well as apparent optical properties such as reflectance, are to a large extent determined by absorption and scattering by pure seawater, and scattering by suspended particles. The present study is focused on the scattering properties of marine particles in the near-IR.

It was shown that if the size distribution of particles found in seawater follows a power-law function, where the number of particles per size bin is a power function of size, and if the particles are non-absorbing, then the spectral distribution of the scattering coefficient is a power function of wavelength [14]. Therefore, in most optical models aimed at predicting light propagation in the ocean, the spectral variations of the particle scattering coefficient are assumed to obey a power function of wavelength, with an exponent that varies between 0 and up to 2 (e.g. [15-16]). It is now well known that this assumption is rarely valid in the visible range because most marine particles are absorbing, i.e. their imaginary part of the refractive index (n') is high enough to impart on the scattering coefficient. This is obviously true for phytoplankton, but as well true for non-algal particles, including mineral ones [2,12]. As a result, a power function of wavelength does not reproduce well observed particle scattering spectra in the visible range (it is often featured in a variable manner), and/or its shape does not reflect in a robust way the particle size spectrum.

In the near-IR, although the imaginary part of the refractive index is probably never absolutely null [11-13], it seems reasonable to us to assume that it is small, if not negligible, relative to the real part of the refractive index for particles (n). Therefore, one may expect that, if the particle size distribution (PSD) does follow a power law, then the spectral variations of the particle scattering coefficient should be a power function of wavelength in the near-IR. Such an assumption has been made in an optical model for discriminating the ocean and atmospheric contributions in reflectance measured at the top of atmosphere (so-called "atmospheric correction") [17]. But in fact, no observation is available at this day to support such a hypothesis. Moreover, the use of the power-law (also called Junge-type) size distribution for marine particles has been challenged by several studies (e.g. [18]).

In this paper, we present the first measurement, to our knowledge, of the marine particle scattering coefficient in the near-IR made on natural samples. Our specific objectives are to:

(i) Determine whether a power law in the form $\lambda^{-\gamma}$, where λ is the wavelength and γ the spectral slope, matches the spectral variations of the scattering coefficient of turbid waters in the near-IR

(ii) If so, document the natural variability of the scattering spectral slope (γ)

(iii) Finally, compare the scattering spectral slope in the near-IR and visible ranges.

To reach these objectives, we measured the light attenuation and absorption coefficients in the visible (412 – 676 nm) and near-IR (715 – 870 nm) spectral regions, in the waters of three different European estuaries.

2. Material and methods

2.1 Field-measurements

An underwater absorption- and attenuation-meter (ac-9, WetLabs, Inc.) was modified to cover the visible and near-IR (700 – 900 nm) spectral regions. It was designed with three visible (440, 555 and 630 nm) and six near-IR (715, 730, 750, 767, 820 and 870 nm) spectral channels, and a short pathlength (10 cm) appropriate for turbid coastal waters.

The measurements were carried out in turbid estuarine waters, namely in the Tamar (South-West UK), Elbe (North Germany) and Gironde (France) estuaries. These waters present high concentrations of non-algal particles (NAP), i.e. fine sediments such as silts and clays. Measurements in the Tamar were carried out onboard the Catfish research vessel (University of Plymouth) on 20 and 24 March, 2005 along two transects between the Plymouth Sound and upstream estuary, over a total of 16 stations. Measurements in the Elbe were first carried out from a pontoon upstream Hamburg (at the limit between the Elbe river and estuary, 3 stations) on 31 October, 2005, then onboard a ferry crossing between Glückstadt and Wischhafen (middle of the estuary, 8 stations) on 1 and 2 November, 2005. In the Gironde, data were collected onboard the Côte d'Aquitaine research vessel during neap tide conditions from 7 to 10 November, 2005 (12 stations), and then during mean and spring tide conditions from 25 to 28 March 2006 (25 stations).

In the Tamar and Gironde, an electrical water pump (SBE, SeaBird, Inc.) was used to carry out ac-9 measurements within the water column. The sensor was first left at five meters deep in order to get rid of air bubbles from the system. The raw attenuation (c_{raw}) and absorption (a_{raw}) signals reached stable values at all wavelengths after less than five minutes. The sensor was then lifted up just below the surface where the ac-9 measurements were recorded during at least two minutes. Temperature and salinity were measured simultaneously using a SeaBird SBE-25 CTD sensor. In the Elbe, the ac-9 sensor could not be deployed into the water from the ferry. Therefore, surface water samples were passed through the ac-9 tubes from the bottom to the top, by gravity (sample container held higher than the instrument), immediately after collection and the a_{raw} and c_{raw} signals were recorded during at least two minutes. Temperature and salinity were measured in the water sample that passed through the ac-9 tubes. The sensor was rinsed after each measurement, and calibrated with Milli-Q water every day in order to obtain a reference signal and verify the instrument stability.

In the moderately turbid waters of the Tamar and Elbe estuaries, measurements of attenuation and absorption were additionally carried out simultaneously using a 25-cm pathlength ac-9 sensor designed with eight visible (412, 440, 488, 510, 532, 555, 630 and 676 nm) and one near-IR (715 nm) channels. The same data acquisition protocol described above for the Tamar and Elbe estuaries was applied.

At all stations, a surface water sample was collected simultaneously with ac-9 measurements. The water was filtered through Whatman Anodisc filters (pore size: 0.2 μm). The reflective (absorption) tube of the ac-9 sensor was then rinsed twice with Milli-Q water, once with the filtrate and finally filled with the filtrate. The absorption signal of the filtrate was measured, providing, after applying corrections for temperature and salinity (see next

paragraph), the absorption coefficient of coloured dissolved organic matter (CDOM) (denoted a_{CDOM}, in m^{-1}).

2.2 Measurement corrections and analyses

The ac-9 data recorded just below the water surface were averaged over the last minute of acquisition to obtain the mean attenuation and absorption spectra for each station. Temperature and salinity corrections were applied to c_{raw} and a_{raw} values to obtain the corrected coefficients, c_{mts} and a_{mts}, respectively [10, 19-20]. With the high attenuation and absorption coefficients measured, the temperature and salinity corrections proved to be very small (typically ranging from 1 to 5% of the measured raw coefficients). In some stations of the Elbe and Gironde estuaries (extremely turbid waters, i.e. c_{raw} >100 m^{-1}), the sensitivity threshold of the ac-9 sensor was reached. As the water turbidity increased, the c_{raw} then a_{raw} signals became very noisy and then saturated around 140 m^{-1} (first at short wavelengths and then progressively at all wavelengths). Similar noise was reproduced when recording ac-9 values with a black cap placed in front of the detectors. In order to avoid significant instrument noise effect on data, we discarded samples with coefficients higher than 100 m^{-1}.

To correct for residual scattering effects on absorption measurements, we applied the "proportional" method developed by [21]. A reference wavelength (λ_{ref}) is used to determine the proportion of the scattering coefficient to be subtracted from the measured a_{mts} signal (Eq. (1)).

$$a(\lambda) = a_{mts}(\lambda) - \frac{a_{mts}(\lambda_{ref})}{c_{mts}(\lambda_{ref}) - a_{mts}(\lambda_{ref})} \times [c_{mts}(\lambda) - a_{mts}(\lambda)] \qquad (1)$$

Where $a(\lambda)$ is the resulting absorption coefficient corrected for temperature, salinity and scattering effects.

The method assumes that there is no spectral dependency of the scattering phase function, which seems to be a valid assumption in turbid waters [14, 22-24]. Several recent studies, however, have suggested [25-26] and even showed [27] contradictory results, i.e. a significant wavelength dependence of the scattering phase function, But, because this study is focused on the scattering coefficient in the near-IR where absorption can be expected to be much smaller than scattering, we believe that possible error in the proportional method had only negligible impact on our calculated scattering coefficients. At the reference wavelength, absorption by substances other than water is assumed null $[a_{mts}(\lambda_{ref}) \equiv 0]$. In this study, the values of the a_{mts} coefficients measured in highly turbid waters with the 10-cm pathlength ac-9 sensor decreased systematically from the visible to the near-IR spectral regions, with a minimal value at 870 nm. Light absorption by CDOM, algal and non-algal particles was assumed to be zero at that wavelength which was used as λ_{ref} in Eq. (1). The 715-nm wavelength was used as λ_{ref} when correcting the few measurements carried out in moderately turbid waters with the 25-cm pathlength ac-9 sensor [e.g. 2].

The scattering coefficient was calculated as the difference between the measured attenuation coefficient corrected for temperature and salinity effects, and the absorption coefficient corrected for temperature, salinity and scattering effects. Those attenuation and absorption coefficients were referenced to pure water. Consequently, the scattering coefficient obtained by difference was also referenced to pure water and, therefore corresponds to the scattering coefficient of marine particulates $[b_p(\lambda)]$:

$$b_p(\lambda) = c_{mts}(\lambda) - a(\lambda) \qquad (2)$$

Errors associated with the final $b_p(\lambda)$ values originate mainly from two sources: (i) photons scattered at small forward angle that are detected and, thus, are not included in the scattering measurement and (ii) multiple-scattering of photons which increases the average pathlength of photons along the tubes (see [28] for detailed definitions). The latter is likely to increase with increasing turbidity. Based on three-dimensional Monte-Carlo radiative transfer simulations,

few studies attempted to estimate the extent of such errors in highly scattering environments [28-29]. They both studied a configuration similar to an ac-9 spectrophotometer with 10 cm pathlength. Using the Petzold phase function at 550 nm [30], results indicate a maximum underestimation of $b_p(\lambda)$ by 26%, related to the first error mentioned above [28]. In [29], also considering the Petzold phase function, the underestimation of $b_p(\lambda)$ ranges from 20% ($c = 1$ m^{-1}) to 27% ($c = 100$ m^{-1}) almost independently of the spectral region (visible and near-IR). Thus, assuming no spectral dependency of the scattering phase function, those studies suggest limited errors (< 25%) on $b_p(\lambda)$ measurements. The increase in pathlength with increasing turbidity is small (< 10% when $b_p = 100$ m^{-1}). Finally, the error on the spectral shape of $b_p(\lambda)$ is also low (typically less than 10%) [29]. Thus, according to these results, the spectral dependency of $b_p(\lambda)$ in turbid coastal waters can be assessed safely from our measurements.

3. Results and discussion

Statistics on the $b_p(\lambda)$ values obtained from ac-9 measurements carried out in the Tamar, Elbe and Gironde are presented in Table 1. The lowest b_p values were observed in the Tamar (mean of about 8 m^{-1} at 715 nm). The highest ones were measured in the Elbe and Gironde estuarine waters (mean of about 46 m^{-1} at 715 nm). Large variations were observed in each estuary.

Table 1. Statistics on the $b_p(\lambda)$ values obtained from ac-9 measurements at selected visible and near-IR wavelengths. Normality of distributions was verified successfully using a Kolmogorov-Smirnov test on log-transformed data. The geometric standard deviation (SD) is to be applied as a factor.

Estuary	b_p (m^{-1})			
	minimum	arithm. mean	maximum	SD
Tamar				
555 nm	1.50	9.48	21.82	2.19
715 nm	1.25	7.85	19.00	2.03
767 nm	1.20	7.49	18.35	1.94
870 nm	1.08	6.78	17.08	2.28
Elbe				
555 nm	3.75	52.16	92.77	2.67
715 nm	3.70	47.19	86.40	2.68
767 nm	3.69	45.76	84.38	2.59
870 nm	3.60	42.95	80.44	3.21
Gironde				
555 nm	11.54	45.65	96.96	1.86
715 nm	9.82	45.91	92.16	1.80
767 nm	9.42	40.47	90.10	1.80
870 nm	8.55	38.27	88.28	1.90

3.1 Spectral dependence of the scattering coefficient

As observed in previous studies [2, 31-32], the measured $b_p(\lambda)$ values decrease with increasing wavelength (Fig. 1). In the Tamar (Fig. 1(a)), large variations of the scattering spectral slope are obvious. In the Elbe (Fig. 1(b)) but also Gironde during neap tide conditions (Fig. 1(c)), these variations are less significant. Also, values of $b_p(\lambda)$ at short wavelengths ($\lambda <$ 555 nm) are lower than would be expected for a $\lambda^{-\gamma}$ spectral distribution. In the Gironde estuary during spring tides, significant variations of the scattering spectral slope can be observed (Fig. 1(d)). The small number of visible channels does not resolve the possible effect of absorption by algal pigments on scattering [2]. In the near-IR, $b_p(\lambda)$ always shows a continuous and smooth decrease with increasing wavelength.

The size distribution of marine particles is often assumed to be well described by a power function of the particle diameter (see [33] and references therein). The exponent of this function is the differential slope (*j*). For non-absorbing spherical particles of constant

refractive index, that follow a power-law distribution between null and infinite diameter, the scattering spectral slope γ is related to the differential slope (j) of the PSD through [14]:

$$\gamma = j - 3 \tag{3}$$

Equation (3) is not valid when n' is significantly larger than zero, and even more when n' shows strong spectral variations. Both are likely not to occur in the near-IR. Therefore, spectral dependence of the scattering coefficient in the near-IR can be assumed to follow the simple power law:

$$b_p(\lambda) = b_p(715) \, (\lambda / 715)^{-\gamma} \tag{4}$$

Where λ and γ are respectively the wavelength and the scattering spectral slope in the near-IR spectral domain (715 – 870 nm). For each station, Eq. (4) was fitted to the measured $b_p(\lambda)$ spectrum by minimising the weighted square sum of the differences between the modelled (Eq. (4)) and measured $b_p(\lambda)$ values. The 715, 730, 750, 767, 820 and 870-nm channels were considered and γ was allowed to vary in the range (-2, 2). This yielded an estimate of the near-IR spectral slope (γ) (Table 2).

Table 2. Statistics on the near-IR (715 – 870 nm) spectral slope (γ). Normality of distributions was verified successfully using a Kolmogorov-Smirnov test. Determination coefficient (R^2) of the power law (Eq. (4)) fitting on measured $b_p(\lambda)$ spectra. Average absolute and relative deviations (in m^{-1} and %, respectively) from the model.

Estuary	Tamar	Elbe	Gironde
near-IR γ spectral slope min.	0.29	0.14	0.12
mean	0.76	0.45	0.45
max.	1.20	0.71	0.72
stdev	0.21	0.18	0.14
R^2 (Eq. (4)) min.	0.994	0.922	0.983
mean	0.997	0.985	0.996
max.	0.999	0.999	0.999
stdev	0.002	0.264	0.004
Average absolute deviation (m^{-1})	0.034	0.074	0.089
Average relative deviation (%)	0.74	0.30	0.24

In the Tamar, γ varied significantly in the range (0.29 - 1.20) (Fig. 2(a)), with a mean value of 0.76 (Table 2). The determination coefficient for the fit of Eq. (4) on data was always larger than 0.99 and deviation from the model was lower than 0.04 m^{-1} (or 0.75%).
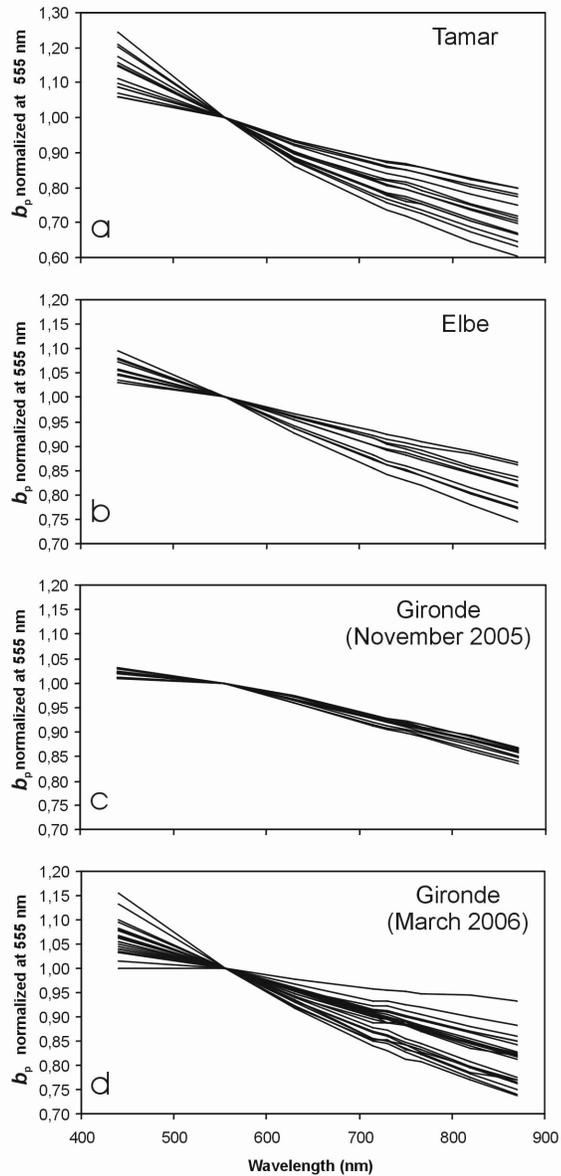
Fig. 1. $b_p(\lambda)$ spectra measured in the Tamar (a), Elbe (b) and Gironde (c) estuaries in October 2005, and in the Gironde (d) estuary in March 2006. Spectra are normalised at 555 nm.

In the Elbe, measurements carried out upstream Hamburg (almost freshwater from the Elbe River) and within the estuary were considered separately. The first ones showed low variability in γ with values around 0.14 (Fig. 2(b)). Equation (4) also applied but with lower determination coefficients (minimum R^2 of 0.92). In the estuary, γ values were higher and presented significant variations in the range [0.25 – 0.71], with a mean value around 0.52. Equation (4) reproduced well the measured $b_p(\lambda_{\text{near-IR}})$ spectra ($R^2 > 0.99$, deviation lower than 0.08 m^{-1} (or 0.30%) from the model in the considered spectral range). The overall Elbe dataset gives a mean γ value of 0.45 (Table 2).

As in the Elbe, values of the γ slope in the Gironde estuary varied in the range (0.12 – 0.72) with a mean value of 0.45 (Figs. 2(c) and 2(d)). Fitting Eq. (4) yielded $R^2 > 0.98$ and deviation from the model was lower than 0.09 m^{-1} (or 0.25%) (Table 2). Tidal conditions seemed to influence the spectral slope of the scattering coefficient. During neap tides (Fig. 2(c)), γ presented very limited variations around the mean value of 0.38. During spring tides (Fig. 2(d)), this mean value slightly increased (0.49) and γ presented significant variations. These variations may result from changes in the PSD in the surface waters (e.g. resuspension of large particles by strong tidal currents). Based on Eq. (3), the γ values obtained from our measurements lead to variations of the differential slope (j) in the ranges (3.29 – 4.20), (3.25 – 3.71) and (3.12 – 3.72), in the Tamar, Elbe and Gironde estuaries, respectively. Such size distributions are expected for marine particle populations [34-37]. Thus, our results validate Eq. (4) for marine particles, in a spectral region where n' is most probably very small [11-13]. These first results suggest that relevant information on the PSD may be obtained from b_p measurements in the (715 – 870 nm) near-IR spectral region when applying Eq. (4), provided that the Junge-type size distribution actually applies to the observed marine particles. Many studies suggest that this is in fact rarely the case (e.g. [18]). Nevertheless, even if the Junge-type distribution does not strictly apply to marine particles, variations in γ may still carry useful information about particle size as shown by [38] for the attenuation coefficient of particles (c_p, m^{-1}).

Equation (4) is not expected to be valid in the visible spectral region due to particulate absorption effects (n' becomes significant compared to n, especially at short visible wavelengths in the case of mineral particles) [2]. We used our dataset to determine how different the particulate scattering spectral slopes are in the visible and near-IR regions. Assuming Eq. (4) to be valid, it was fitted to the b_p values measured at 440, 555, 630 and 715 nm. Results (Table 3) show that spectral variations of b_p in the visible region are rather well reproduced with a power law but a significant departure from Eq. (4) was also often observed (R^2 coefficient as low as 0.61, deviation of 0.11 to 0.16 m^{-1} from the model in the considered spectral range). The most striking result is the significant difference between the visible and near-IR scattering spectral slopes. It was systematically lower in the visible region (respectively 17%, 29% and up even 49% lower in the Tamar, Gironde and Elbe estuaries). A clear conclusion that can be drawn from those results with regard to optical modelling, is that measurements of particle scattering made in the visible cannot be safely extrapolated over the near-IR. The latter must be documented directly. This is a major contribution of the present study.
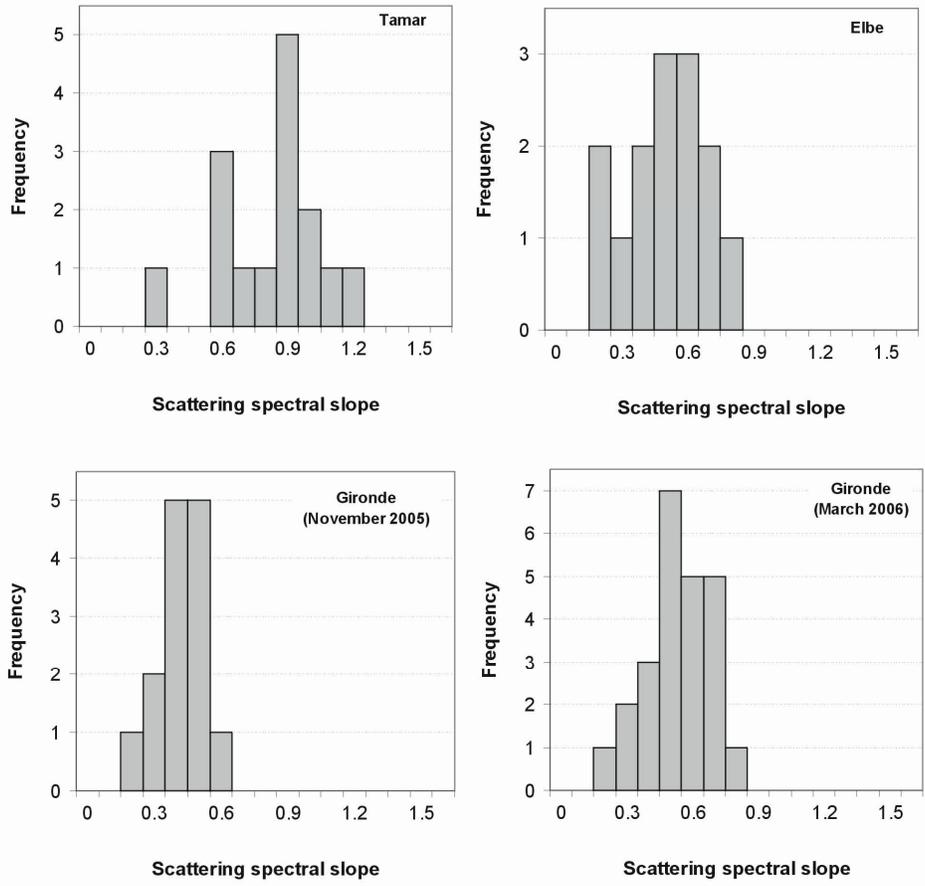
Fig. 2. Scattering coefficient spectral slope (exponent γ in Eq. (4)) observed in the near-IR (715 – 870 nm) spectral region. Measurements made in the Tamar, Elbe, and Gironde estuaries in November 2005, and in the Gironde estuary in March 2006, are presented separately.

Table 3. Statistics on the visible (440 – 715 nm) spectral slope (γ). Normality of distributions was verified successfully using a Kolmogorov-Smirnov test. Determination coefficient (R^2) of the power law (Eq. (4)) fitting on measured $b_p(\lambda)$ spectra. Average absolute and relative deviations (in m^{-1} and %, respectively) from the model.

Estuary		Tamar	Elbe	Gironde
Visible γ spectral slope	**min.**	0.21	-0.18	0.11
	mean	0.63	0.23	0.32
	max.	1.04	0.44	0.63
	stdev	0.23	0.22	0.13
R^2 (Eq. (4))	**min.**	0.670	0.609	0.788
	mean	0.961	0.829	0.949
	max.	0.997	0.990	1.000
	stdev	0.082	0.157	0.049
Average deviation (m^{-1})		0.109	0.127	0.159
Average absolute deviation (%)		0.96	0.51	0.42

We now look at the relationship between γ in the near-IR and $b_p(715)$. The rationale is that changes in $b_p(715)$ largely reflect changes in the load of particles in suspension. $b_p(715)$ is high when resuspension processes are active and, possibly, favour the occurrence of larger particles. When it is low, one may expect smaller particles to dominate as they remain in suspension longer than large ones. Because changes in γ reflect changes in the size of particles (Eq. (3)), there may exist a relationship between γ and $b_p(715)$. Such a relationship was observed in the bottom boundary layer of a continental shelf [38]. Note that this may be true for $b_p(\lambda)$ at any wavelength, but even more in the near-IR where the scattering coefficient is *a priori* not much affected by absorption effects (i.e. by n'). Such a relationship would be useful in the modelling of seawater optical properties.

No correlation between γ and $b_p(715)$ was found in the Tamar and Gironde (Fig. 3). In the Elbe estuary, a clear trend of decreasing γ values with increasing $b_p(715)$ is observed if the measurements in the Elbe freshwater are considered as an exception (the three points at low $b_p(715)$ and γ). When considering all data together, a general trend of decreasing spectral slopes γ when $b_p(715)$ is increasing appears (Fig. 3). Based on Eq. (3), it would suggest the predominance of fine particles in moderately turbid waters (the Tamar) and coarser particles in highly turbid waters (the Elbe and the Gironde) possibly due to flocculation processes. But this general trend shows high dispersion.
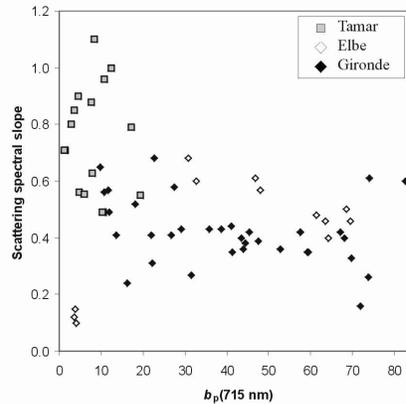
Fig. 3. Plot of the scattering spectral slope (γ) between 715 and 870 nm as a function of $b_p(715)$ in the Tamar, Elbe and Gironde estuaries.

3.2 Spectral slopes of the particulate attenuation and scattering coefficients

As already observed and explained [2], the spectral variations of $b_p(\lambda)$ depart from the $\lambda^{-\gamma}$ power law when light absorption by particles becomes significant relatively to scattering ($n' > 0$). This may occur at short visible wavelengths ($\lambda < 550$ nm) for mineral and detrital particles (actual b_p values at lower wavelengths tend to be smaller than what a $\lambda^{-\gamma}$ spectral distribution would suggest), and/or around phytoplankton pigment absorption bands. This was confirmed in the present study (see Tables 2 and 3, and text above). However, a $\lambda^{-\gamma}$ spectral dependency may still be expected for the particulate attenuation coefficient because of compensating variations in a_p and b_p [38]. In coastal waters dominated by detritus and resuspended sediments, where light scattering was predominant over absorption at all visible (412 – 676 nm) wavelengths, a $\lambda^{-\gamma cp}$ spectral dependency (similar to the one defined by Eq. (4)) on the particulate attenuation coefficient (c_p in m^{-1}, sum of the particle absorption and scattering coefficients, a_p and b_p, respectively) was observed by [38]. The associated spectral slope (γ_{cp}) was found to covary with the differential slope (j) according to Eq. (3). Based on these results, this differential slope could be retrieved directly from the spectral slope of $c_p(\lambda)$. This would be convenient as measurements of the beam attenuation coefficient are less prone to error compared to scattering measurements, especially in the visible range.

Using our dataset, we compared the near-IR scattering spectral slope to the visible spectral slope of the particulate attenuation coefficient in order to confirm this assumption. We considered as reference the spectral slope of b_p in the near-IR spectral region (715 – 870 nm), denoted γ. It was compared to the spectral slope of the particulate attenuation coefficient in the visible region, denoted γ_{cp}, i.e. the spectral slope considered in [38]. The first aim was to determine how significantly light absorption by particles influences the spectral slope of the particulate attenuation coefficient. The second step was to assess the resulting error when using the attenuation slope to retrieve information about the PSD using Eq. (4). One must keep in mind that the analysis that follows, which is based on our measurements, relies upon three assumptions: (i) no spectral dependence of the scattering phase function (Eq. (1)); (ii) no light particulate absorption at 870 nm, and (iii) a PSD following a power-law function with an infinite size distribution and constant spectral n.

The c_p coefficient was obtained by subtracting the absorption coefficient of the dissolved fraction (a_{CDOM}) from the total attenuation signal (c):

$$c_p(\lambda) = c(\lambda) - a_{CDOM}(\lambda) \qquad (5)$$

For all samples, the spectral slope γ_{cp} was calculated from the c_p coefficients measured with the 10-cm ac-9 sensor at 440, 555, 630 and 715 nm. For some of the samples

(moderately turbid waters of the Tamar and Elbe estuaries), γ_{cp} was also calculated from the c_p coefficients measured with the 25-cm ac-9 sensor at 412, 440, 488, 510, 532, 555, 630 and 676 nm, in order to strictly reproduce the protocol previously adopted [38]. The obtained γ_{cp} slopes were finally compared to γ (Fig. 4). Results indicate that γ_{cp} is systematically higher than γ, and by 27, 17 and 15% on average, in the Tamar, Gironde and Elbe estuaries, respectively (Fig. 4(a)). If the three assumptions mentioned above were valid, this would indicate that light absorption by particles was significant in the three estuaries in the (440 – 715 nm) spectral region, and that the use of $c_p(\lambda)$ instead of $b_p(\lambda)$ does not completely eliminate the effect of n' on spectral variations of scattering. If shorter wavelengths are considered, i.e. the 412 – 676 nm spectral region [38], γ_{cp} is further higher than γ (on average 57% for the Tamar-Elbe dataset). Thus, the use of γ_{cp} to estimate j may lead to a slight but significant overestimation of the latter. This overestimation remains limited if only wavelengths longer than 440 nm are considered, which tends to validate the approach recently proposed [38,39]. But the overestimation can increase dramatically if short visible wavelengths are used.
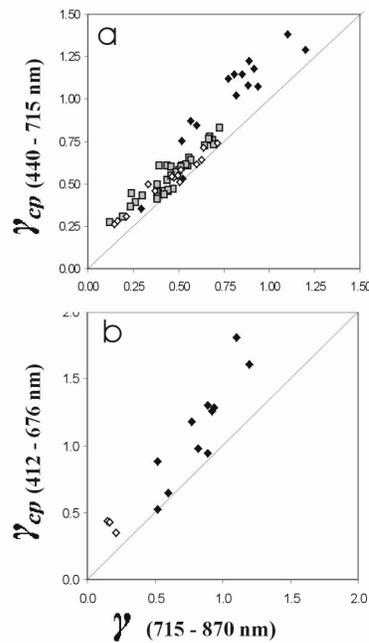

Fig. 4. Plot of the particulate attenuation coefficient spectral slope γ_{cp} in the 440 – 715 nm (a) and 412 – 676 nm (b) spectral ranges as a function of the particulate scattering spectral slope γ in the 715 – 870 nm near-IR spectral region. Solid lines show the 1:1 relationships. Black, grey and white points represent the Tamar, Gironde and Elbe data, respectively.

Finally, it is of interest to examine whether the spectral behavior of c_p and b_p are similar in the near-IR (which is expected to be true in the case of non-absorbing particles [38]) and also to assess the influence of the correction applied for residual scattering (see Eq. (1)) on the result. The c_p and b_p spectral slopes proved to be much similar in the (715 – 870 nm) region ((Fig. 5(a)). However, once again, γ_{cp} was systematically higher than γ, by 7, 8 and 11% on average, in the Tamar, Gironde and Elbe estuaries, respectively. This could be expected as light absorption (by particles and dissolved organic matter) was observed to be low but significant at 715 nm and assumed to be null at 870 nm. This explains the slight difference between the c_p and b_p spectral slopes (9% on average).
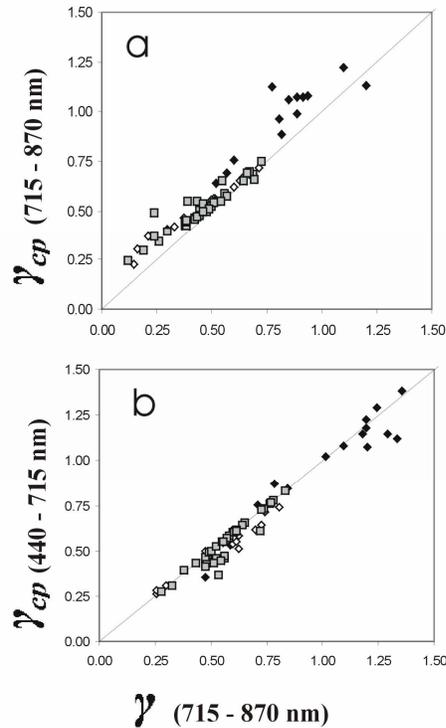
Fig. 5. Plot of the particulate attenuation coefficient spectral slope γ_{cp} as a function of the particulate scattering spectral slope γ in the 715 – 870 nm near-IR spectral region (a). Plot of γ_{cp} in the 440 – 715 nm visible spectral region as a function of γ in the 715 – 870 nm near-IR spectral region, when assuming no light absorption by particles and coloured dissolved organic matter at 715 nm and longer wavelengths (b). Solid lines show the 1:1 relationships. Black, grey and white points represent the Tamar, Gironde and Elbe data, respectively.

If light absorption by particles and coloured dissolved organic matter is assumed to be null at 715 nm and longer wavelengths (i.e. considering 715 nm as λ_{ref} in Eq. (1) which corrects absorption measurements for residual scattering effects), the γ_{cp} slope in the visible (440 – 715 nm) spectral region is almost equal to γ (with a normalized root mean squared deviation lower than 3.5% on average) (Fig. 5(b)). Under this assumption, c_p and b_p are equal in the near-IR (715 – 870 nm) spectral region and have, obviously, the same spectral slope. The selection of 715 nm rather than 870 nm as λ_{ref} in Eq. (1) only induces a slight (+7% on average) increase of the γ values presented in Table 2. Thus, while it cannot be concluded from our study that light absorption by particles is significant between 715 and 870 nm, the values obtained for the γ slopes in this spectral region are most probably good estimates. Based current knowledge, there is much uncertainty about absorption by marine particles beyond 750 nm (e. g. [13]), but it is quite clear that the assumption of null light absorption by particles at 715 nm is not valid. The use of 870 nm as λ_{ref} in Eq. (1) seems more reasonable, but is still an assumption to be validated.

4. Conclusions

Simultaneous field measurements of light attenuation and absorption coefficients carried out in three estuaries using a WetLabs ac-9 sensor modified to cover the near-IR spectral region (715 – 870 nm) were used to determine the near-IR spectral variations of the particle scattering coefficient. A simple power law ($\lambda^{-\gamma}$) closely reproduced these spectral variations

(mean R^2 of 0.99). As expected in the visible spectral region, a significant departure from this power law was observed. The near-IR spectral slope (γ) varied in the range (0.1 – 1.2). Significant variations of γ were observed (mean values of 0.76, 0.45 and 0.45 in the Tamar, Elbe and Gironde estuaries, respectively). These variations certainly reflect significant changes in the PSD. This assumption needs to be confirmed based on simultaneous b_p and PSD field measurements.

Results presented in this study will be useful for bio-optical modelling purposes (propagation of light in the ocean) and to develop ocean colour algorithms for turbid coastal waters (e.g. quantification and determination of the size distribution of particles). They notably have implications for atmospheric corrections of ocean colour data [17, 40-41] dealing with the discrimination of aerosols and hydrosols optical signatures. Whether the observed variations in γ are significant or not with regards to atmospheric corrections over turbid waters remains to be determined. The inherent optical property directly influencing ocean colour remote sensing measurements is the particulate backscattering coefficient (b_{bp}). The results presented in this study are expected to be relevant to remote sensing applications as the particulate backscattering ratio (b_{bp}/b_p) has apparently no significant spectral dependence in natural waters (at least in the visible spectral region) [24].

Acknowledgments